Chinese Journal of
POLYMER SCIENCE

RESEARCH ARTICLE

https://doi.org/10.1007/s10118-026-3669-7
Chinese J. Polym. Sci.

Iodine-mediated Atom Transfer Radical Polymerization Enabled by the Cooperative Reverse Iodine Transfer Polymerization and Reversible Complexation Mediated Polymerization

Meng-Qi Ge[a], Xin-Wei Chen[a], Liang Wu[a], Xiang-Yi Wang[a], Ning Ren[a*], and Xin-Yuan Zhu[a,b*]

[a] *School of Chemistry and Chemical Engineering, State Key Laboratory of Polyolefins and Catalysis, Research Institute of Polymer Materials, Shanghai Jiao Tong University, Shanghai 200240, China*
[b] *Frontiers Science Center for Transformative Molecules, Shanghai Jiao Tong University, Shanghai 200240, China*

Electronic Supplementary Information

Abstract Iodine is an attractive candidate for living radical polymerization owing to its strong halogen bonding ability and the vigorous C—I bond, enabling diverse mechanisms including iodine transfer polymerization (ITP), reverse iodine transfer polymerization (RITP), reversible complexation mediated polymerization (RCMP), and atom transfer radical polymerization (ATRP). Among them, iodine-mediated ATRP stands out for its high activation rate constants, low equilibrium constants, and convenient post-polymerization modification. However, the use of alkyl iodides as initiators remains challenging because they are thermally and photochemically unstable. To solve this question, RITP mechanism was incorporated into the ATRP for the *in situ* generation of the alkyl iodide from I_2. Further studies revealed that the ATRP ligands could also trigger the RCMP mechanism. Kinetic studies, radical trap experiments, and density functional theory (DFT) calculations clarified the contributions of each mechanism. This RITP/RCMP/ATRP ternary polymerization avoids the use of unstable initiators and achieves controlled polymerization of various monomers.

Keywords Reverse iodine transfer polymerization (RITP); Reversible complexation mediated polymerization (RCMP); Atom transfer radical polymerization (ATRP); Reversible deactivation radical polymerization (RDRP); Ternary polymerization

Citation: Ge, M. Q.; Chen, X. W.; Wu, L.; Wang, X. Y.; Ren, N.; Zhu, X. Y. Iodine-mediated atom transfer radical polymerization enabled by the cooperative reverse iodine transfer polymerization and reversible complexation mediated polymerization. *Chinese J. Polym. Sci.* https://doi.org/10.1007/s10118-026-3669-7

INTRODUCTION

Iodine is a promising candidate for reversible deactivation radical polymerization (RDRP), which requires the establishment of a dynamic equilibrium between the propagating radicals and the dormant species.[1–9] The uniqueness of iodine arises primarily from its relatively weak C—I bond. Taking benzyl halides as an example, the bond-dissociation energies (BDEs) of C—Cl and C—Br are about 71.6 and 57.2 kcal/mol, respectively, whereas the BDE for C—I bond is only 44.9 kcal/mol, facilitating the activation of C—I bond during the polymerization.[10–12] In addition, because of its larger polarizability, iodine can form stronger halogen bonding interactions with electron-rich species than chlorine and bromine,[13] which enhances its compatibility with organic catalysts including organic amines, super bases, iodide anions, *etc.*[4,6] Iodine-terminated polymers also demonstrate significant advantages in post-polymerization modification.[14–17] These features allow iodine to participate in several RDRP methods, including iodine transfer polymerization (ITP)[3,9,18,19], reverse iodine transfer polymerization (RITP)[3,9,18,20,21], reversible complexation mediated polymerization (RCMP)[4,6,22], reversible chain transfer catalyzed polymerization (RTCP)[23–25] and atom transfer radical polymerization (ATRP)[2,8,26], as summarized in Scheme 1.

In (R)ITP, the controlled chain growth is achieved by the equilibrium between the propagating radical and the dormant P_n-I.[3,9,18,19] While ITP uses alkyl iodides as chain transfer agents, RITP uses molecular iodine (I_2) and thermal initiator to generate alkyl iodide *in situ* because alkyl iodides are less stable.[3,9,18,20,21] However, the relatively slow chain transfer rate of iodine restricts both ITP and RITP, making it difficult for the polymerization to reach low dispersity.[27,28]

To improve the transfer efficiency between the propagating radical and the dormant P_n-I, RTCP and RCMP were developed by Goto *et al.*, who used different agents to facilitate iodine exchange.[4,6,22–25] In RTCP, the organic iodides act as deactivators that can promote rapid degenerative chain transfer with propagating radicals, enabling a frequent iodine

* Corresponding authors, E-mail: ningren@sjtu.edu.cn (N.R.)
E-mail: xyzhu@sjtu.edu.cn (X.Y.Z.)
Received February 26, 2026; Accepted March 16, 2026; Published online June 26, 2026

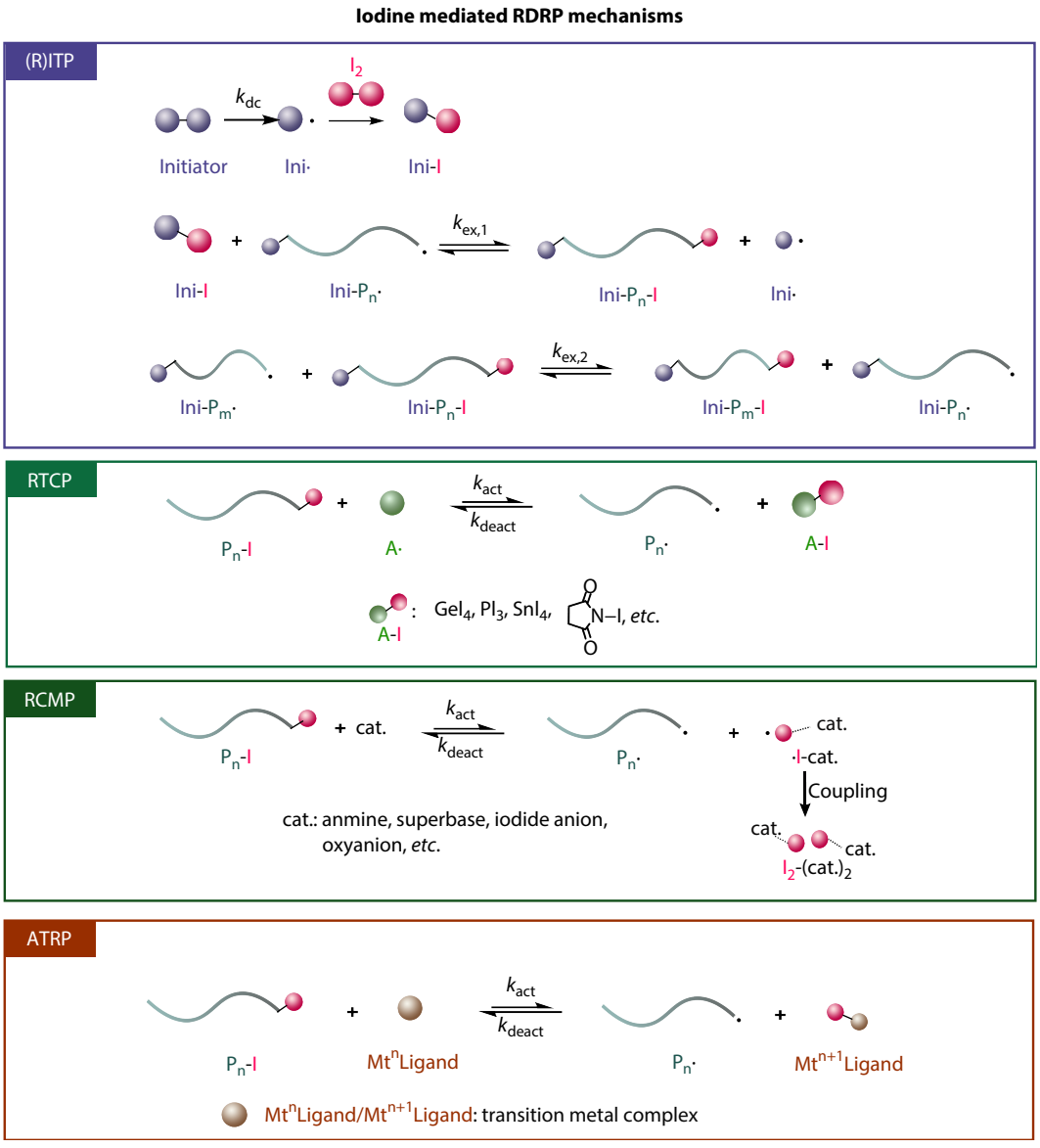

Scheme 1 Iodine mediated RDRP mechanisms.

transfer reaction and well-controlled polymerization.[25] A wide variety of Ge-[25,29], Sn-[25,29], P-[25,30], N-[25,31], O-[32], and C-[32,33] centered organic iodides have been demonstrated to mediate this process. External radicals are required to initiate polymerization and activate organic iodides. However, the activator generated from the organic iodides may combine with $P_n^{\bullet}$, resulting in the formation of dead chains and the reduction in polymerization rates.[34,35] In contrast to RTCP, RCMP relies on the halogen bonding interaction between organic molecules (*e.g.*, amines[4,22,36], super bases[4,37], Schiff bases[4,38], iodide anions[4,39–41], oxyanions[4,42], *etc.*) and alkyl iodides to achieve controlled polymerization. During RCMP, organic molecules can directly activate alkyl iodide initiators *via* reversible complexation, efficiently generating radicals *in situ* without the need for external radical initiators.[22,43] Nevertheless, owing to insufficient accumulation of deactivators at the early stage of polymerization, I_2 often needs to be added externally to maintain the livingness of polymerization.[22,36,43]

The high reactivity of iodine also makes it appealing for ATRP, enabling fast activation/deactivation processes that help maintain livingness and facilitate post-polymerization modification.[2,8,15,26] Compared to bromine and chlorine, iodine-mediated ATRP exhibits higher activation rate constants (k_{act}) and lower equilibrium constants (K_{ATRP}). For example, for initiator with the structure X-CH(CH_3)$COOCH_3$ (X=I, Br, or Cl), the k_{act} values are 0.53, 0.33, and 0.015 L·mol^{-1}·s^{-1}, for iodine, bromine, and chlorine respectively, while the corresponding K_{ATRP} values are 2.2×10^{-8}, 3.8×10^{-8}, and 3.2×10^{-7}, respectively.[44,45] This indicates that iodine ATRP promotes a faster activation and deactivation process, which is beneficial for controlled polymerization.[2,26] Matyjaszewski *et al.* reported that polymers with dispersity ($Đ$) of only 1.10–1.15 could be obtained by ATRP using methyl 2-iodopropionate and CuI.[26] In addition, Anastasaki *et al.* found that Cu(0) could also be used to activate alkyl iodide initiating RDRP under mild

conditions.[2] The polymers obtained with ethyl 2-iodo-2-methylpropionate as initiator under ambient temperature showed controlled polymerization with M_n ranging from 10^3 Da to 10^5 Da with $Đ$ as low as 1.06.[2] Beyond polymerization, iodine-terminated polymers exhibit advantages in post-polymerization modification, enabling efficient azidation and thiol-halogen click reactions at reduced reagent or catalyst loadings relative to bromine-terminated polymers.[14–17]

Nevertheless, the use of alkyl iodides in RTCP, RCMP, and ATRP still faces challenges. Because of the relatively low C—I BDE, alkyl iodides are prone to decomposition under light or heat, thereby complicating the storage and handling.[18,46] To overcome this limitation, prior work on RTCP and RCMP has combined RITP to generate alkyl iodide initiators *in situ*. This strategy avoids the use of unstable iodide initiator and offers inspiring insights into iodine-mediated polymerization.[25,41,43,47,48] Inspired by the pioneering work of Goto and Wang, we attempted to integrate the RITP mechanism into ATRP, in which alkyl iodide initiators are generated *in situ* from thermal initiators and I_2 during polymerization, eliminating the need for pre-synthesized unstable alkyl iodides. The generated alkyl iodides can then initiate ATRP with copper complex. Controlled polymerization can be achieved with various monomers under different copper sources. Further mechanistic investigation revealed that the ATRP ligand can also trigger the RCMP process through the ligand-iodine complexation, establishing a ternary mechanism interplay of RITP, RCMP and ATRP (Scheme 2). To further elucidate the mechanism, the contributions and interactions of the three methods at different polymerization stages were studied: the initiators were generated from I_2 and thermal initiator through RITP, the polymerization rate was tuned by the complexation of P_n-I and ligand through RCMP, and the controlled polymerization was ensured by the combination of Cu^I/ligand activation (ATRP) and I_2 deactivation (RITP). This study established a new iodine-mediated controlled radical polymerization framework and demonstrated the potential of combining complementary mechanisms. We believe that this research advances the understanding of multi-mechanism RDRP and expands the scope of iodine-mediated controlled polymerizations.

EXPERIMENTAL

The details can be found in the electronic supplementary information (ESI).

RESULTS AND DISCUSSION

ATRP with *In situ* Generated Initiator *via* RITP

As shown in Fig. 1, to incorporate RITP into ATRP, the alkyl iodide initiator (2-iodo-2-methylpropanenitrile, CPI) can be generated *in situ* by the decomposition of 2,2'-azobis(2-methylpropionitrile) (AIBN) and the radical capture of I_2. The generated CPI can serve as the ATRP initiator. The equilibrium between the propagating radicals and dormant chains was established through multiple activation-deactivation pathways to enable controlled polymerization. ATRP with an *in situ* formed initiator requires six essential components: monomer, thermal initiator, I_2, cupric salt, ligand, and solvent. As shown in Fig. 1, the monomers employed in this work are methyl methacrylate (MMA), butyl methacrylate (BMA), isobutyl methacrylate (IBMA), benzyl methacrylate (BzMA), poly(ethylene glycol) methacrylate (PEGMA), and lauryl methacrylate (LMA). CuI is investigated using pentamethyldiethylenetriamine (PMDETA) as the ligand.

Table 1 summarizes the results of the iodine-mediated ATRP of various monomers using CuI as the copper source. Polymerizations of MMA, IBMA and BzMA with CuI (Table 1, Runs 1–3) proceed in a controlled manner, yielding polymers with low dispersity ($Đ$=1.19–1.28). Similarly, the controlled polymerization of LMA (Table 1, Run 4) is achieved at a lower monomer concentration ([monomer] = 1 mol/L). For BMA and PEGMA, polymerizations are conducted at 60 °C with 2,2'-azobis-(2,4-dimethylvaleronitrile) (ABVN) as thermal initiator, where the alkyl iodide initiator 2-iodo-2,4-dimethylpentanenitrile (ACI) is generated *in situ via* the reaction of ABVN with I_2.

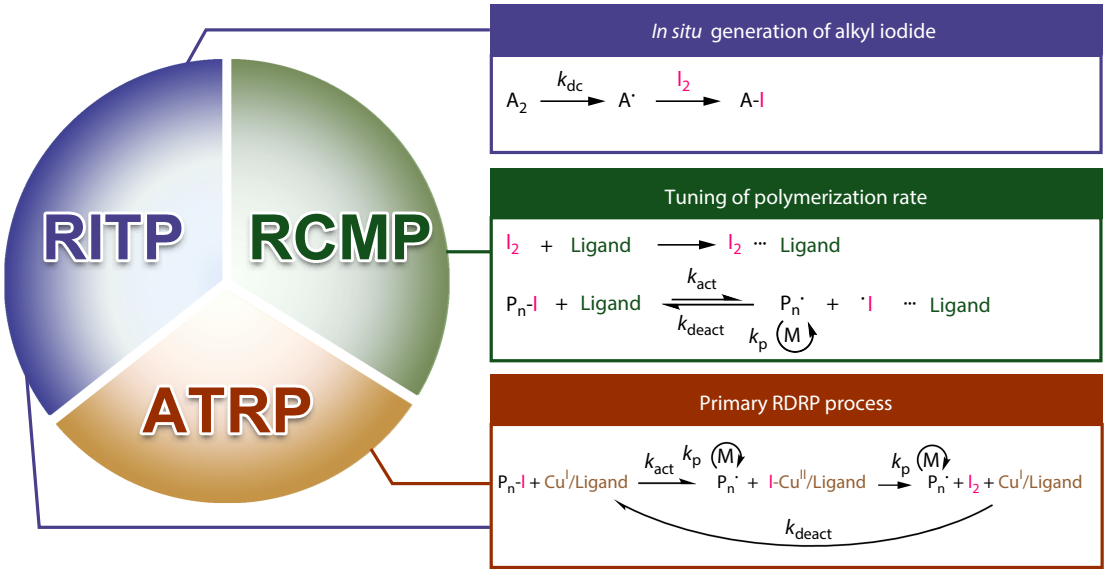

Scheme 2 Ternary polymerization with RITP, RCMP and ATRP.

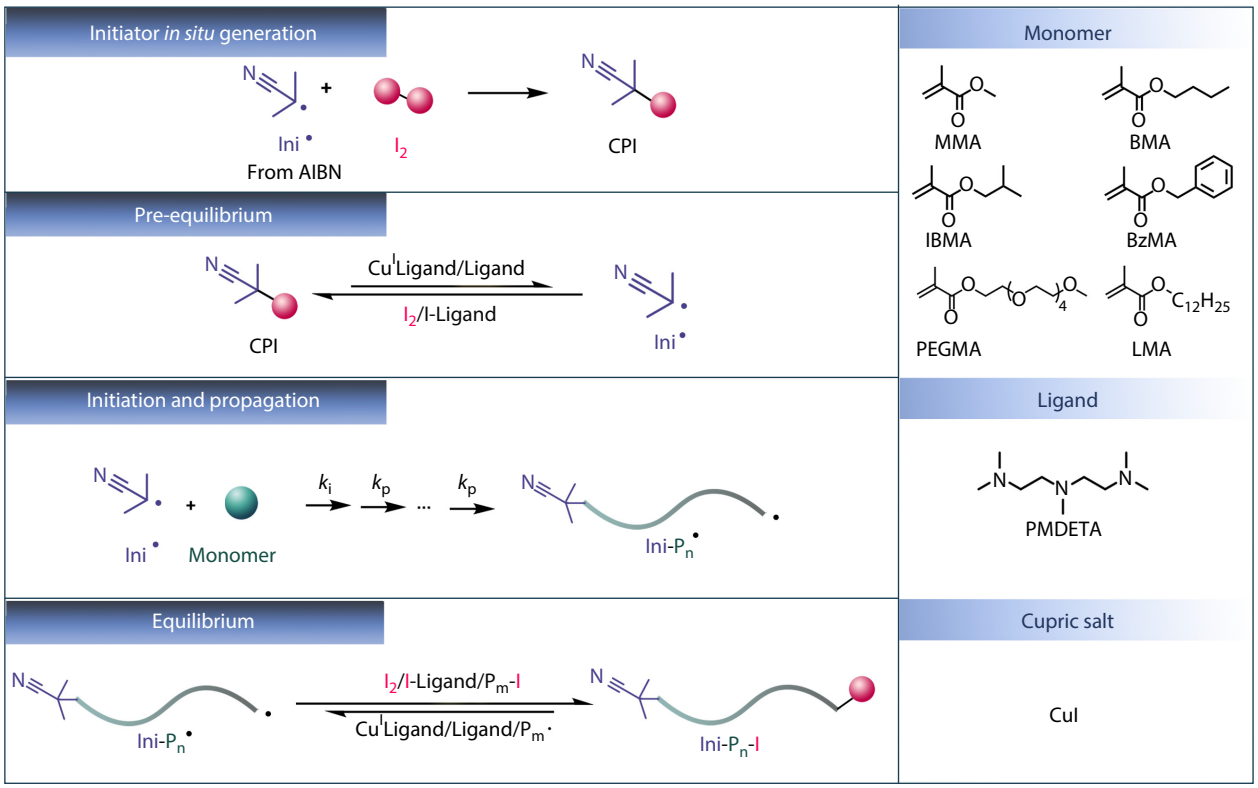

Fig. 1 Demonstration of polymerization process and substrates used in the polymerization.

Table 1 Controlled polymerization of various monomers with CuI/PMDETA as metal complex. [a]

Run	Monomer	*t* (h)	Conv. [b]	$M_{n,theo}$ [c] (kDa)	$M_{n,SEC}$ (kDa)	*Đ*
1	MMA	7	75%	7.7	7.9	1.25
2	IBMA	6	70%	10.2	12.9	1.28
3	BzMA	6	77%	13.8	14.3	1.19
4	LMA [d]	8	77%	17.5	18.0	1.23
5 [e]	BMA	8	72%	10.4	9.6	1.13
6 [e]	PEGMA [d]	9	76%	23.1	19.8	1.28

[a] Conditions: [monomer]: [I_2]: [AIBN]: [CuI]: [PMDETA] = 200:1:2:0.4:0.4, all polymerizations were conducted at 75 °C with [monomer] = 3 mol/L in toluene with 5% *N*,*N*-dimethylformamide (DMF) (*V*/*V*); [b] Monomer conversion was determined by ^{1}H-NMR; [c] $M_{n,theo} = \frac{[M]}{2[I_2]} \cdot M_M \cdot \text{Conv.} + M_{CPI}$ for Runs 1–4, $M_{n,theo} = \frac{[M]}{2[I_2]} \cdot M_M \cdot \text{Conv.} + M_{ACI}$ for Runs 5 and 6; [d] [monomer] = 1 mol/L; [e] Polymerization was conducted at 60 °C using ABVN as the thermal initiator.

Under this condition, both BMA and PEGMA exhibit controlled polymerizations with low dispersity (Table 1, Runs 5 and 6), especially for BMA (*Đ*=1.13). In addition, kinetic analysis through proton nuclear magnetic resonance (^{1}H-NMR) under these conditions shows pseudo-first-order behaviors and a linear increase of M_n with monomer conversion (Figs. S1–S7 in the electronic supplementary information, ESI). These results demonstrate that iodine-mediated ATRP polymerization exhibits good livingness across various monomers. In addition, MMA polymerization targeting different degrees of polymerization can be conducted in a controlled manner within appropriate conversion ranges (Fig. S8 in ESI).

The repeating unit and end-group of the synthesized polymer were analyzed by Fourier transform ion cyclotron resonance mass spectrometry (FT-ICR MS) and ^{1}H-NMR using the polymerization of MMA with CuI/PMDETA as the model reaction. The target DP was set to 50 to allow for the accurate determination of the end-group *via* FT-ICR MS. Fig. 2(a) and Fig. S9 (in ESI) display a series of MMA peaks separated by 100.05 Da. In FT-ICR MS spectrum (Fig. 2a), peak A is assigned to iodine-terminated PMMA. Peaks B and C are attributed to lactone- and alkene-terminated PMMA, respectively. These signals originate from the transformation of iodine-terminated PMMA during FT-ICR MS analysis because of the liability of the halogen terminals.[49,50] The NMR spectra (Fig. 2b) also confirm the end-group structure. The peak between 3.70–3.76 ppm (peak 4 in Fig. 2b) corresponds to the methyl protons of the iodine terminals.

Polymerization Mechanism

As iodine was used to construct the ATRP, other mechanisms could also exist during the propagation, including iodine-mediated degenerate chain transfer from RITP and reversible complexation between the ligand and I_2/P_n-I from RCMP (Scheme 2). To understand the polymerization mechanism, a series of control experiments were performed, including independent

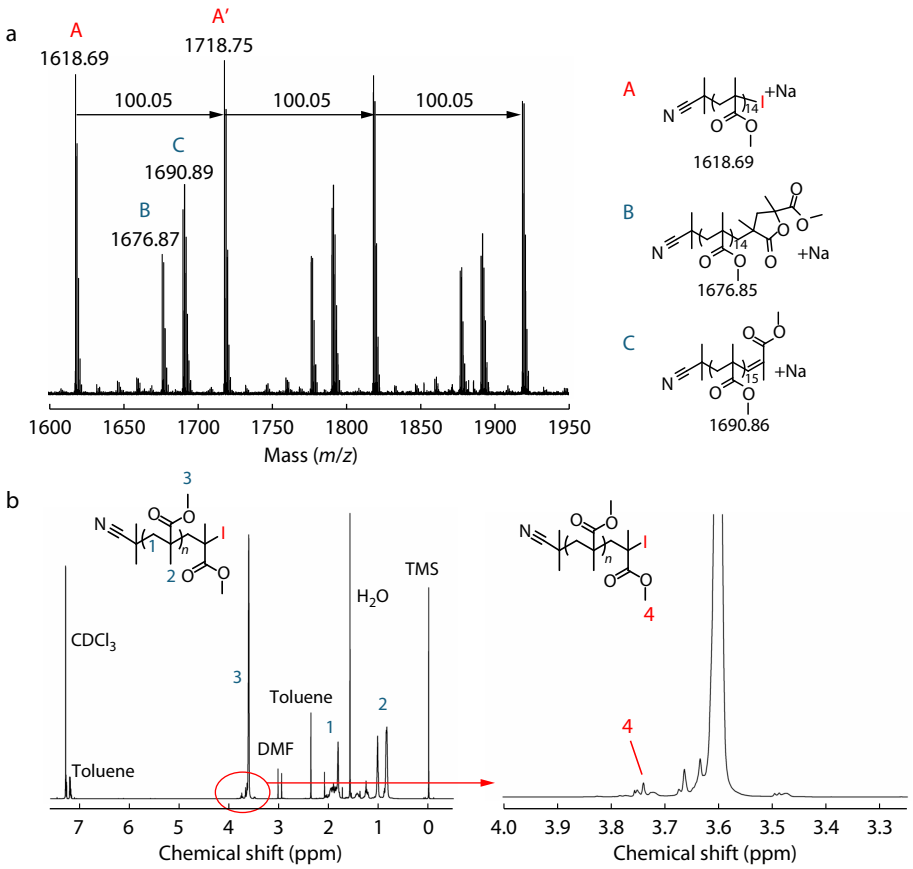

Fig. 2 (a) FT-ICR MS spectrum of PMMA; (b) ^{1}H-NMR spectra with $CDCl_3$ as solvent of PMMA. ([MMA]:[I_2]:[AIBN]:[CuI]:[PMDETA] = 100:1:2:0.4:0.4).

mechanisms (RITP and RCMP) and combined binary mechanisms (RITP/RCMP and RCMP/ATRP), as shown in Table 2. These experiments aimed to elucidate the origin of the living behavior by comparing the effects of independent and combined mechanisms.

Polymerization initiated by I_2 in the absence of ligand and copper represented an independent RITP process, in which alkyl iodides were generated *in situ via* radical trapping and subsequently regulated polymerization through reversible iodine transfer. However, this polymerization exhibits poor livingness with a high dispersity (*Đ*=1.93, Table 2, Run 1, Fig. S10 in ESI). According to reference, without the help of ligand or copper complex, the low chain transfer rate of iodine between propagation radicals is inefficient for establishing the dynamic equilibrium.[19,27,28,41] In contrast, polymerization conducted with pre-synthesized CPI in the presence of ligand but without copper corresponds to the independent RCMP pathway, where the ligand reversibly complexed with CPI and P_n-I to facilitate iodine exchange without involving the *in situ* generation of CPI. Nevertheless, poor controlled polymerization is also observed with *Đ*=1.73 (Table 2, Run 2, Fig. S10 in ESI) due to insufficient accumulation of the deactivator (I_2-amine complex) at the early stage of polymerization.[36]

Because both independent RITP and RCMP were unable to afford the controlled polymerization of MMA, the combination of these two mechanisms was further examined. When I_2 and ligand were simultaneously introduced, RITP and RCMP proceeded concurrently, combining *in situ* alkyl iodide generation and iodine transfer with ligand-mediated reversible complexation of iodine species. Previous studies have demonstrated that the combination of RITP and RCMP enables the controlled polymerization of MMA with tetrabuty-

Table 2 Control experiments to evaluate the contribution of independent and combined mechanisms in the iodine-mediated ATRP. [a]

Run	Mechanism	Initiation	Ligand	*t* (h)	Conv. [b]	$M_{n,theo}$ (kDa) [c]	$M_{n,SEC}$ (kDa)	*Đ*
1 [d]	RITP	I_2	–	11	70%	7.2	9.8	1.93
2 [e]	RCMP	CPI	PMDETA	6	72%	7.4	7.2	1.73
3 [f]	RITP+RCMP	I_2	PMDETA	5	75%	7.8	9.0	1.61
4 [g]	RCMP+ATRP	CPI	PMDETA	7	75%	7.8	6.3	1.41

[a] All polymerizations were conducted at 75 °C with [MMA] = 3 mol/L in toluene with 5% DMF (*V*/*V*); [b] Monomer conversion was determined by ^{1}H-NMR; [c] $M_{n.theo} = \frac{[MMA]}{2[I_2]} \times M_{MMA} \times Conv. + M_{CPI}$ for Runs 1 and 3; $M_{n.theo} = \frac{[MMA]}{[CPI]} \times M_{MMA} \times Conv. + M_{CPI}$ for Runs 2 and 4; [d] [MMA]:[I_2]:[AIBN] = 200:1:2; [e] [MMA]:[CPI]:[AIBN]:[PMDETA] = 200:2:0.2:0.4; [f] [MMA]:[I_2]:[AIBN]:[PMDETA] = 200:1:2:0.4; [g] [MMA]:[CPI]:[AIBN]:[CuI]:[PMDETA] = 200:2:0.2:0.4:0.4.

https://doi.org/10.1007/s10118-026-3669-7

lammonium iodide or triethylamine as organic molecules.[41,43,47] Wang *et al*. also reported that for a classic RCMP without thermal initiator, the external addition of 20% I_2 (relative to initiator) can act as supplemental deactivators in the presence of PMDETA for the polymerization of MMA.[36] However, for binary RITP/RCMP polymerization with initiator generated by I_2 and AIBN, the use of PMDETA only slightly improved the livingness with $Đ$=1.61 (Table 2, Run 3, Fig. S10 in ESI), which is consistent with a previous report.[36]

The coexistence of CPI, ligand, and CuI led to binary RCMP/ATRP polymerization, where alkyl iodides participate in both ligand- and copper-mediated iodine transfer equilibria. As shown in Table 2, Run 4, when PMDETA is employed as the ligand, binary RCMP/ATRP yields polymers with $Đ$=1.41 (Fig. S10 in ESI). This high dispersity could arise from the absence of I_2, which can serve as the dormant species to control radical concentration.[8,9,19] An independent ATRP is not included because the ligands required for ATRP inevitably promote RCMP through reversible complexation.

The above control experiments demonstrate that independent RITP, RCMP, binary RITP/RCMP, and RCMP/ATRP can all conduct polymerization of MMA, but the control of each polymerization remains limited. This indicates that a combination of all three mechanisms is essential for achieving controlled polymerization. Scheme 3 summarizes the proposed polymerization mechanism involving the cooperative operation of the three pathways. During the induction stage, CPI is first generated through a radical reaction between I_2 and the thermal initiator, following the RITP pathway. As I_2 is gradually consumed and CPI accumulates, polymerization enters the propagation stage, where CPI serves as the initiator species that can be activated either by the Cu(I)/ligand through the ATRP pathway or by the ligand through the RCMP pathway. During propagation, polymerization is mainly regulated by two dynamic equilibria: ligand-mediated RCMP equilibrium and ATRP activation combined with I_2-based RITP deactivation. In this stage, ATRP provides efficient activation of the C—I bond, while I_2 rapidly deactivates propagating radicals, forming a dominant ATRP/RITP activation-deactivation cycle. Meanwhile, RCMP modulates the activation rate through ligand-iodine complexation. In contrast, the contribution of iodine transfer *via* RITP remains limited due to the inherently slow transfer rate of iodine.[27,28] To further verify the mechanism, polymerization of MMA was used as the model reaction for investigation.

In situ generation of CPI and induction period

The *in situ* generation of CPI *via* the RITP process leads to an induction period prior to propagation (Fig. S1 in ESI) because the rapid coupling of radicals with I_2 predominates over monomer addition at an early stage.[51–53] *In situ* NMR was used to study this process. Figs. 3(a) and 3(b) present the kinetic data of CPI and monomers under different polymerization mechanisms according to the NMR spectra (Figs. S11 and S12 in ESI). The results in Fig. 3(b) show that the induction period does exist in independent RITP, binary RITP/RCMP, and ternary RITP/RCMP/ATRP polymerizations. The initiation period was divided into two stages. In Stage 1, CPI is continuously generated and gradually reaches its maximum with nearly no monomer consumption. As the concentration of I_2 significantly decreases, radical-iodine coupling becomes less competitive than monomer addition, representing the end of the induction period (Stage 1) and the start of initiation and propagation (Stage 2).

During Stage 1, significant differences exist between different polymerizations, considering both the apparent generation rate and the maximum concentration of CPI (Fig. 3a, Stage 1). In the independent RITP, CPI is generated at a larger apparent rate constant (4.7×10^{-4} mol·L^{-1}·min^{-1}, Fig. S13 in ESI) than that in binary RITP/RCMP and ternary RITP/RCMP/ATRP, reaching the maximum concentration of 1.02×10^{-1} mol/L and the longest induction period of about 200 min (Figs. 3a and 3b). As illustrated in Fig. 3(c), the use of ligands converts the independent RITP mechanism into binary RITP/RCMP polymerization by complexing with I_2 and CPI. Complexation between the amine and I_2 hindered the generation of CPI while accelerating its activation. Both processes contribute to a smaller apparent generation rate constant

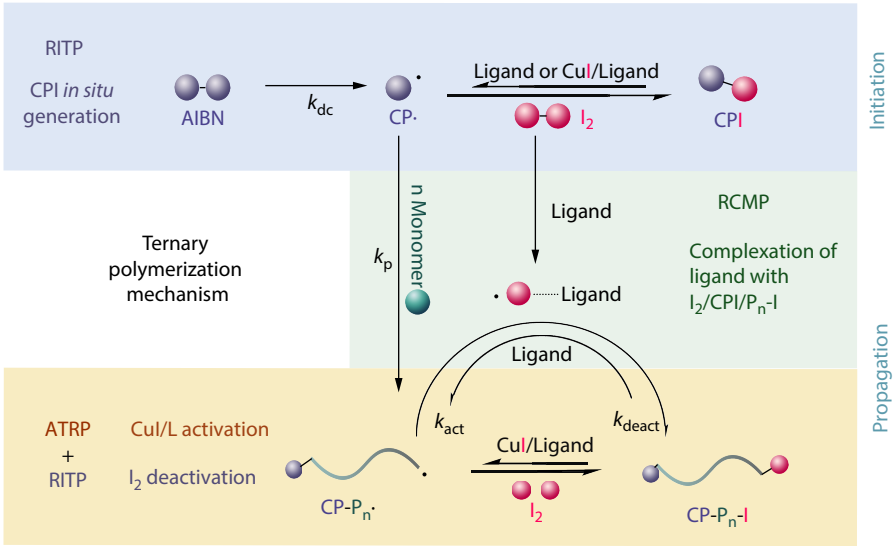

Scheme 3 Ternary polymerization with RITP, RCMP and ATRP.

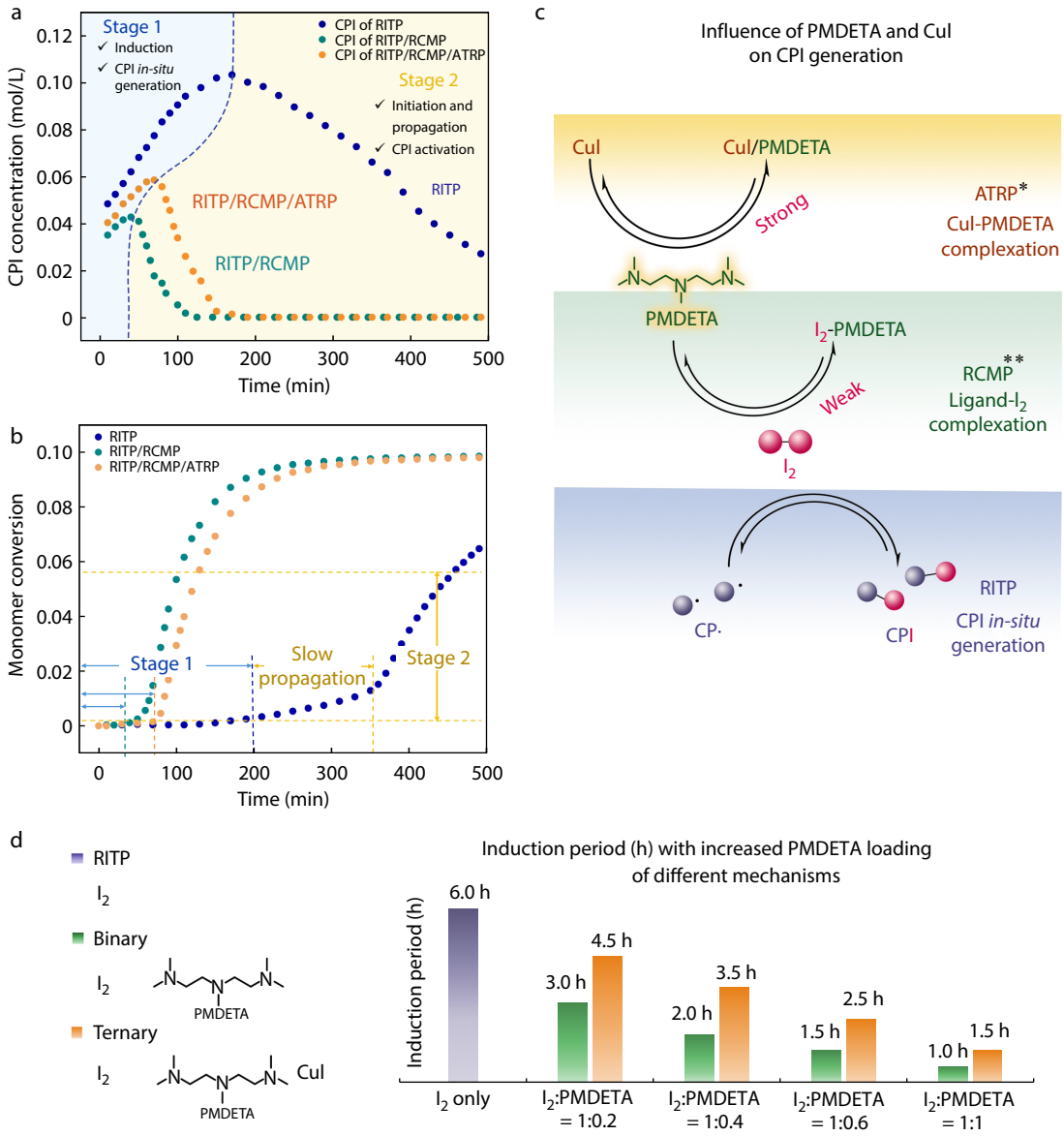

Fig. 3 (a) Evolution of CPI concentration versus time for different mechanisms; (b) MMA conversion versus time for different mechanisms (blue for RITP, green for binary RITP/CMP, yellow for ternary RITP/RCMP/ATRP); (c) Demonstration of CPI generation pathway influenced by PMDETA and CuI (* CPI can be activated by CuI; ** CPI can also be activated by PMDETA); (d) Induction period of independent RITP, binary RITP/RCMP and ternary RITP/RCMP/ATRP with increased PMDETA loading.

(3.31×10^{-4} mol·L^{-1}·min^{-1}) of CPI and a reduced maximum CPI concentration (4.27×10^{-2} mol/L), leading to a shortened induction period (approximately 40 min).

For ternary RITP/RCMP/ATRP polymerization with both the amine ligand and CuI, the generation of CPI during Stage 1 is governed by the interplay among the three mechanisms (Fig. 3c). The Cu^{I} exhibits strong complexation ability with the amine ligand (equilibrium constant log K=6.53 for Cu^{I} + PMDETA ⇌ Cu^{I}-PMDETA complex), whereas the complexation of I_2 with amine is much weaker (equilibrium constant log K=3.67 for I_2 + triethylamine ⇌ I_2-triethylamine complex).[54,55] Density functional theory (DFT) calculations also confirmed the lower energy of ligand-copper complexation compared to that of ligand-I_2 (Fig. S14 in ESI). These results indicate that PMDETA has a much higher affinity for Cu^{I} than for I_2. Consequently, PMDETA predominantly complexes with Cu^{I}, which limits its interaction with I_2 and reduces the generation of iodine-ligand complexes during Stage 1. As a result, the induction period is prolonged compared to the binary RITP/RCMP mechanism (70 min), and the maximum CPI concentration increases to 5.84×10^{-2} mol/L with a larger apparent CPI generation rate constant (3.80×10^{-4} mol·L^{-1}·min^{-1}, Fig. S13 in ESI). However, compared with the independent RITP, both the CPI apparent generation rate constant and its maximum concentration are still lower. This is because both Cu^{I} and the free ligand can activate CPI, thereby accelerating its consumption. Consequently, the ternary RITP/RCMP/ATRP achieves a slightly higher maximum CPI concentration than the binary RITP/RCMP, while remaining largely below that of the independent RITP mechanism (Fig. 3a). Correspondingly,

the induction period exhibits an intermediate duration between the binary RITP/RCMP and the independent RITP mechanism, as shown in Fig. 3(b).

To further confirm the influence of the ligand and copper complex on CPI generation, we comparatively analyzed the variations of the induction period in binary RITP/RCMP and ternary RITP/RCMP/ATRP mechanisms ([CuI]: [I_2] = 0.4:1) at different ligand concentrations (Fig. 3d). In both cases, the induction period gradually shortens with increasing ligand concentration, indicating that ligand-iodine complexation affects both the generation and consumption of CPI. Increased ligand-iodine interactions suppress CPI generation while facilitating consumption once it is formed. Consistent with this analysis, polymers obtained from both binary RITP/RCMP and ternary RITP/RCMP/ATRP polymerizations exhibit higher molar masses with increasing PMDETA loading at comparable monomer conversions (Table 3, Runs 2–5 and 7–9), indicating that higher ligand concentrations reduce the effective amount of CPI generated in the induction period.

An exception is observed in ternary polymerization when the ligand content is lower than that of copper (Table 3, Run 6). Under this condition, the amount of ligand is insufficient to fully coordinate all copper species, resulting in a reduced concentration of active Cu-ligand complexes. Consequently, the activation-deactivation exchange becomes kinetically inefficient, leading to poor control with high dispersity ($Đ$=1.86). Notably, the ternary polymerization exhibits a longer induction period than the binary RITP/RCMP, because most of the ligands are complexed with copper, reducing its availability for iodine complexation and thereby enhancing the generation of CPI. Correspondingly, comparisons between Table 3 Runs 3 and 7, Runs 4 and 8, and Runs 5 and 9 reveal that, at the same ligand loading and similar conversion, the ternary polymerization RITP/RCMP/ATRP affords polymers with a lower molar mass than the binary RITP/RCMP, confirming a relatively higher CPI concentration in the ternary RITP/RCMP/ATRP process.

Activation of CPI and initiation/propagation

After the induction period, the CPI generated can be activated by different mechanisms, producing radicals to initiate polymerization (Fig. 4a). For independent RITP, the CPI generated during the induction period is subsequently activated solely through iodine transfer with radicals from the AIBN decomposition and propagating chains. Owing to the low transfer efficiency of iodine,[27,28] its activation rate constant is rather small (2.57×10^{-3} min^{-1}, Fig. 4b), which also limits the overall apparent polymerization rate constant (6.29×10^{-4} min^{-1}, Fig. 4c). However, in RITP/RCMP binary polymerization, the halogen bonding interaction between the ligand and iodine atom enables the rapid activation of CPI. The results in Fig. 4(b) show that, compared to independent RITP, the presence of the RCMP mechanism significantly enhances the apparent consumption rate constant of CPI by 13.3 times. The introduction of the ligand also accelerates the overall activation-deactivation dynamics, and the rate constant of binary RITP/RCMP polymerization is enhanced by roughly 31.6 times when compared with RITP polymerization (Fig. 4c).

When CuI and the ligand are both introduced to form the ternary RITP/RCMP/ATRP polymerization, the CPI activation rate constant decreases by 22% compared to the binary RITP/RCMP polymerization, although it remains much larger than that in independent RITP. This trend is consistent with earlier observations of CPI generation, where the preferential complexation of the ligand with Cu^{I} limits its complexation with CPI *via* the RCMP mechanism. The relatively small activation rate constant of CPI leads to a reduced radical concentration, thereby lowering the apparent polymerization rate constant (1.65×10^{-2} min^{-1}), yet it still exceeds that of independent RITP (Figs. 4b and 4c).

The effect of ligand loading on propagation (Stage 2) was also studied. As shown in Figs. 4(d) and 4(e), the apparent polymerization rate constants increase with higher ligand loading in both binary and ternary polymerizations, which is consistent with the trend observed for the induction period. In binary RITP/RCMP, a higher ligand concentration can enhance the CPI activation rate through the RCMP mechanism and facilitate the reactivation of dormant chains, leading to a higher radical concentration and faster polymerization. Considering the complexity of multi-mechanism radical polymerization,[56,57] the binary kinetic model was adopted to further verify this trend (Table S3 in ESI).[58–62] As [Ligand]/[I_2] increases from 0.2 to 1.0, the hybrid constants for the binary RITP/RCMP ($\varphi_{RCMP/RITP}$) remain negative, and their absolute values progressively increase. The negative φ values indicate that the presence of RCMP exerts a synergistic effect on the independent RITP mechanism, thereby enhancing its propagation rate. However, elevated radical concentration can also increase the probability of irreversible termination, which can

Table 3 Polymerizations of independent RITP, binary RITP/RCMP and ternary radical polymerization with increased PMDETA loading. [a]

Run	Mechanism	CuI loading [b]	PMDETA loading [b]	t (h)	Conv. [c]	$M_{n,theo}$ [d] (kDa)	$M_{n,SEC}$ (kDa)	$Đ$
1	RITP	–	–	11	70%	7.2	9.8	1.93
2	RITP/RCMP	–	0.2	7	72%	7.4	6.8	1.54
3	RITP/RCMP	–	0.4	5	71%	7.3	9.2	1.57
4	RITP/RCMP	–	0.6	4.5	75%	7.7	9.9	1.61
5	RITP/RCMP	–	1.0	3.5	72%	7.4	12.6	1.77
6	Ternary	0.4	0.2	9	70%	7.2	8.6	1.86
7	Ternary	0.4	0.4	7	75%	7.7	7.9	1.25
8	Ternary	0.4	0.6	5	74%	7.6	8.7	1.31
9	Ternary	0.4	1.0	3.5	71%	7.3	11.4	1.39

[a] All polymerizations were conducted at 75 °C with [MMA]: [I_2]: [AIBN] = 200:1:2, [MMA] = 3 mol/L in toluene with 5% DMF (*V*/*V*); [b] relative to [I_2]; [c] Monomer conversion was determined by ^{1}H-NMR; [d] $M_{n.theo} = \frac{[MMA]}{2[I_2]} \times M_{MMA} \times Conv. + M_{CPI}$.

https://doi.org/10.1007/s10118-026-3669-7

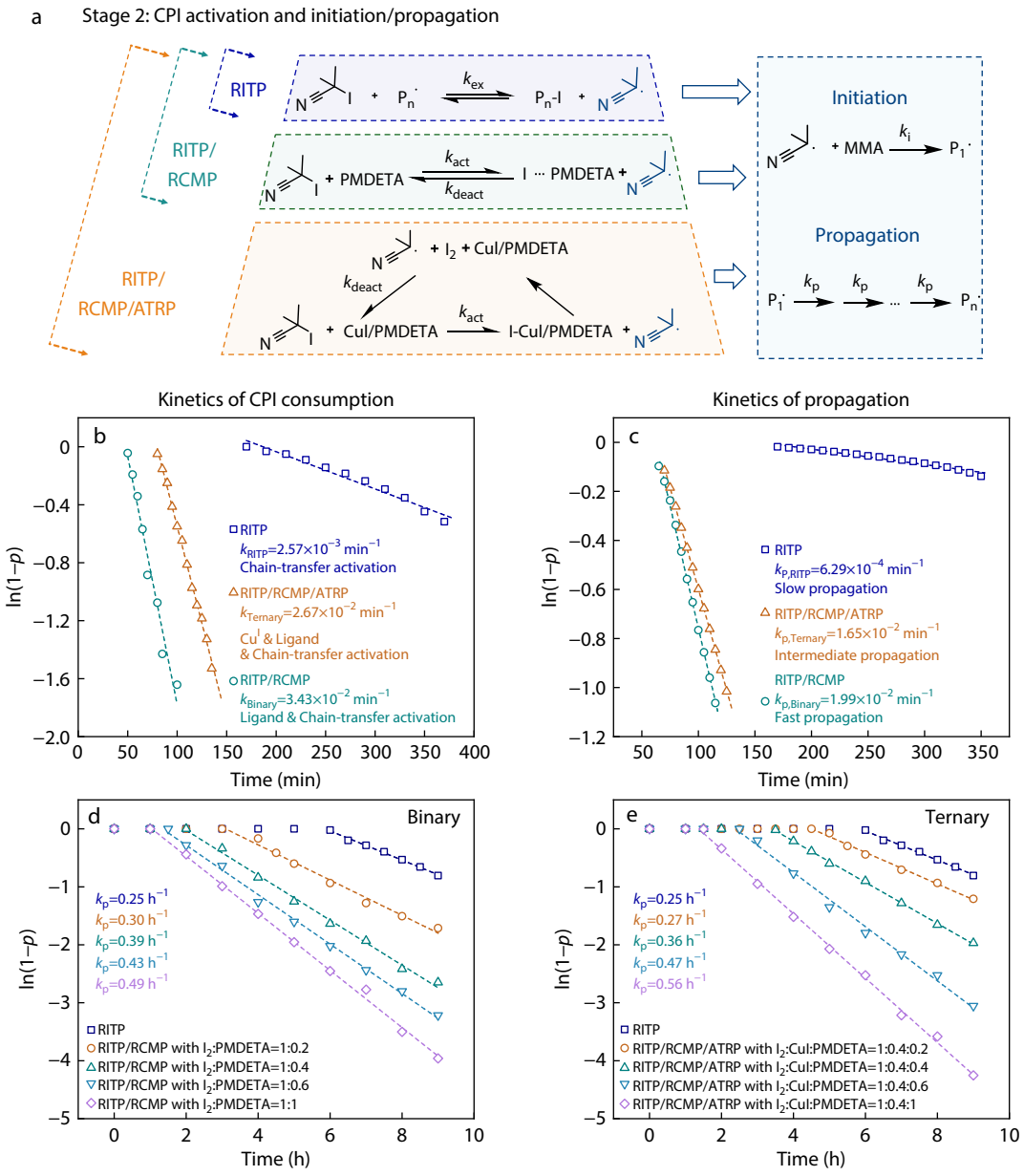

Fig. 4 (a) Activation pathways of CPI *via* RITP, RCMP and ATRP and subsequent initiation/propagation; (b) Kinetic behavior of CPI consumption through *in situ* NMR; (c) Kinetic behavior of monomers through *in situ* NMR (blue: independent RITP, green: binary RITP/RCMP, yellow: ternary RITP/RCMP/ATRP); (d) Kinetic behavior of binary RITP/RCMP polymerization with different ligand loading; (e) Kinetic behavior of ternary RITP/RCMP/ATRP polymerization with different ligand loading.

compromise the livingness of polymerization. Accordingly, the dispersity of the polymers gradually increases with increasing ligand loading (Table 3, Runs 2–5, Fig. S15a in ESI).

In ternary RITP/RCMP/ATRP polymerization, the effect of ligand loading on polymerization is more complex. Although both the polymerization rate constants and the absolute values of the hybrid constants ($\varphi_{(RCMP+ATRP)/RITP}$) increase with ligand concentration, the polymer dispersity exhibits a non-monotonic dependence on ligand loading. When the ligand content is lower than that of copper (Table 3, Run 6), the dispersity is relatively high ($Đ$=1.86) because insufficient ligand limits the generation of copper-ligand complexes, leading to poor control of polymerization and a slower propagation rate. Upon increasing the ligand-to-copper ratio to 1:1 (Table 3, Run 7), nearly all copper species are efficiently complexed and engaged in the ATRP equilibrium. In this way, ATRP dominates the regulation of polymerization, whereas ligand-mediated iodine exchange remains minimal. As a result, the polymerization exhibits improved livingness and lowest dispersity ($Đ$=1.25). Further increasing the ligand loading beyond this ratio (Table 3, Runs 8 and 9, Fig. S15b in ESI), the excess ligand introduces additional effects. First, when the ligand is present in excess relative to copper, the amine ligands can act as reducing agents, facilitating the reduction of Cu^{II} to Cu^{I}, thereby sustaining the continuous generation of activators (Cu^{I}).[63] Second, a higher availability of free ligands enhances

https://doi.org/10.1007/s10118-026-3669-7

reversible complexation with CPI and P_n-I, strengthening iodine transfer *via* the RCMP process. Together, these effects lead to an increase in radical concentration, which results in a higher polymerization rate and a shortened induction period but also causes a gradual increase in dispersity owing to the elevated probability of irreversible termination. Notably, even at increased ligand loadings, the dispersity of ternary RITP/RCMP/ATRP remains lower than that of binary RITP/RCMP, indicating the critical role of CuI in sustaining polymerization livingness. These results demonstrate that a balanced ligand-to-copper ratio (1:1) is essential for ternary polymerization to achieve an optimized propagation rate and livingness, reflecting the complex interplay between the RCMP and ATRP mechanisms.

Iodine-mediated activation-deactivation process via ATRP and RITP

In iodine-mediated ATRP polymerization, the activation-deactivation equilibrium differs from that of the classic bromine-based ATRP. The activation of dormant P_n-I chains by CuI leads to the generation of CuI_2 species. However, unlike $CuBr_2$, CuI_2 is unstable and prone to decomposition, limiting its ability to function as an effective deactivator.[26] This suggests that an alternative deactivation pathway may play a dominant role during the equilibrium stage. Interestingly, Tang *et al.* recently proposed supplemental activation reducing agent (SARA) ATRP activation and I_2 deactivation mechanism.[8] During this SARA ATRP, $FeBr_3$/Fe(0) activates dormant P_n-I into propagating $P_n^{\bullet}$ and generates unstable $FeBr_2I$, which decomposes into $FeBr_2$ and I_2. The *in situ* generated I_2 further deactivates $P_n^{\bullet}$ converting it back to a dormant state.[8]

Inspired by this work, we proposed a mechanism dominated by ATRP activation *via* CuI/L and RITP deactivation *via* I_2 as illustrated in Fig. 5(a). Specifically, dormant chains (P_n-I) are activated by CuI/L, generating propagating radicals ($P_n^{\bullet}$) and the CuI_2/L complex. This complex then decomposes into CuI/L and I_2. The resulting I_2 can act as a radical trapping agent, deactivating $P_n^{\bullet}$ through direct iodine capping, analogous to the CPI generation process in the RITP mechanism. To validate the proposed mechanism by which the activation of P_n-I by CuI leads to the generation of I_2, high-performance liq-

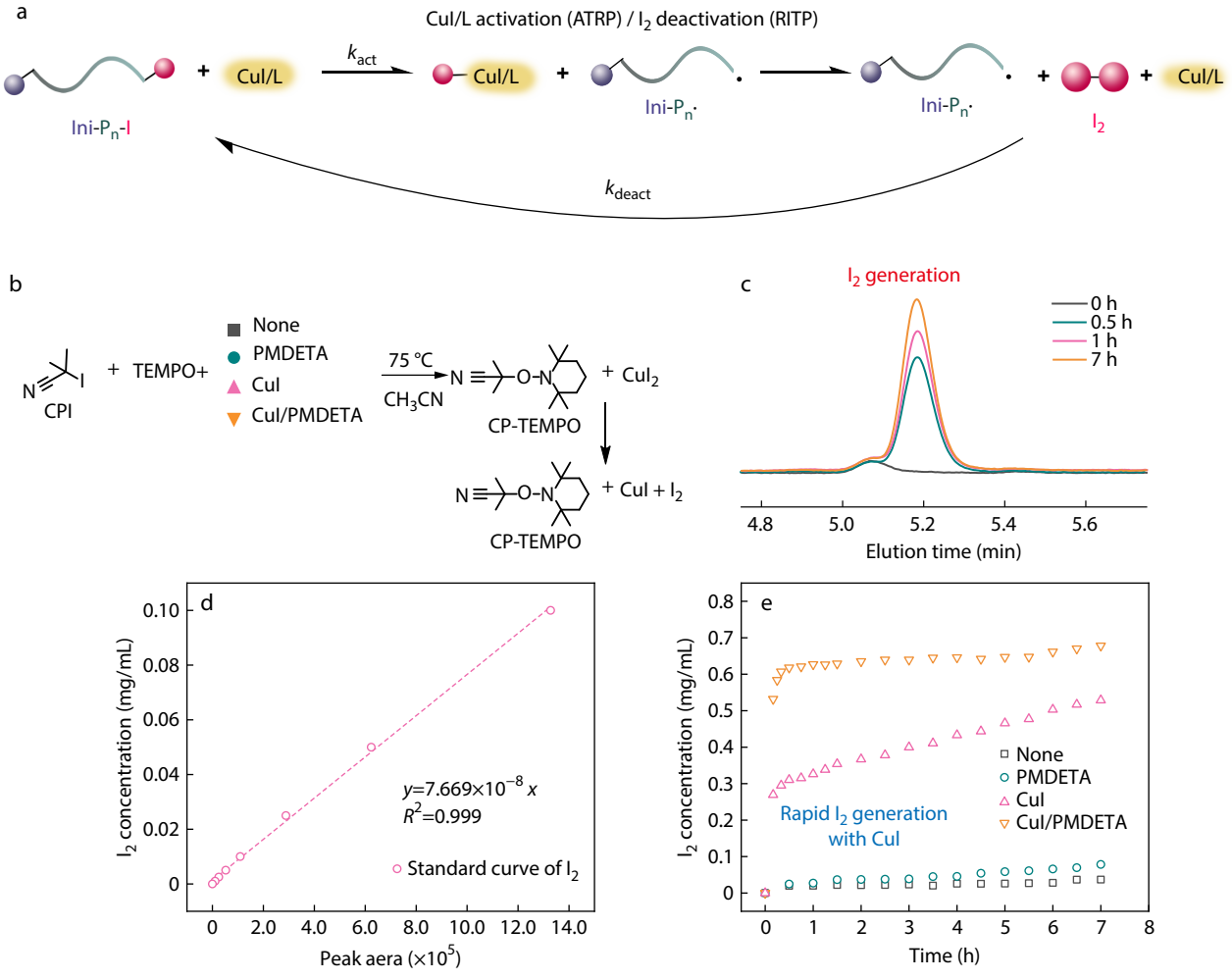

Fig. 5 (a) Proposed mechanism of CuI/L activation (ATRP)/I_2 deactivation (RITP); (b) Radical trap experiments for I_2 generation under different conditions (gray: [CPI]:[TEMPO] = 1:1.5; green: [CPI]:[TEMPO]:[PMDETA] = 1:1.5:1; pink: [CPI]:[TEMPO]:[CuI] = 1:1.5:1; yellow: [CPI]:[TEMPO]:[CuI]:[PMDETA] = 1:1.5:1:1); (c) HPLC spectra of I_2 generation with CPI, TEMPO and CuI; (d) Standard curve of I_2 concentration versus peak aera; (e) I_2 concentration versus time under different conditions.

uid chromatography (HPLC) was employed to monitor the generation and kinetic behavior of I_2. To make the generation of I_2 irreversible and facilitate precise kinetic determination, 2,2,6,6-tetramethylpiperidoxyl (TEMPO) was added as a radical-trapping agent.[8,24,37] As shown in Fig. 5(b), four model reactions were designed to distinguish the effects of copper and ligand: (1) CPI+TEMPO, (2) CPI+TEMPO+PMDETA, (3) CPI+TEMPO+CuI, and (4) CPI+TEMPO+CuI+PMDETA. Fig. 5(c) and Fig. S16 (in ESI) show the HPLC data for the determination of I_2 concentration during the model reaction under different conditions. To quantitatively assess the kinetics of I_2 generation under various conditions, a standard curve correlating the peak area with I_2 concentration was established by analyzing standard solutions of different concentrations under identical HPLC conditions and performing linear regression of peak area versus concentration (Fig. 5d). The standard curve enabled the quantification of I_2 generation kinetics (Fig. 5e).

The results showed that without ligand and copper, the generation of I_2 from CPI decomposition is low, with no more than 3.7×10^{-2} mg/mL (Fig. 5e, gray square). The addition of PMDETA leads to a slight increase in I_2 generation (7.8×10^{-2} mg/mL), likely due to the thermal decomposition of iodine-amine complexes (Fig. 5e, green dot). In contrast, when CuI is added, rapid I_2 generation is observed reaching 5.3×10^{-1} mg/mL in 7 h (Fig. 5e, pink triangle). The use of PMDETA in the model reaction with CuI further accelerates the generation of I_2, with the concentration rising to approximately 6.2×10^{-1} mg/mL within only 0.5 h (Fig. 5e, yellow inverted triangle). These results indicate that efficient I_2 generation occurs in the presence of copper, and the additional PMDETA further promotes this process. This enhancement arised from the lowered Cu^{II}/Cu^{I} redox potential by PMDETA, which facilitates the oxidation of Cu^{I} to Cu^{II}, shifting the equilibrium toward the activation process and consequently accelerating the generation of I_2.[64]

This radical trapping experiment suggests that, in the proposed ternary RITP/RCMP/ATRP polymerization, the activation of P_n-I by CuI can lead to the generation of I_2, which further deactivates the radicals forming P_n-I. It should be mentioned that, besides this ATRP process, iodine transfer *via* both RITP and RCMP can affect the livingness of polymerization. However, because the direct chain transfer ability of iodine is weak,[27,28] the contribution of RITP through degenerate chain transfer in the propagation process is limited and is thus ignored in the latter discussion. To further elucidate the contributions of copper-based ATRP, I_2-based RITP, and ligand-based RCMP, DFT calculations were performed using MMA as the monomer, CuI as the copper source, and PMDETA as the ligand. All DFT calculations were performed using

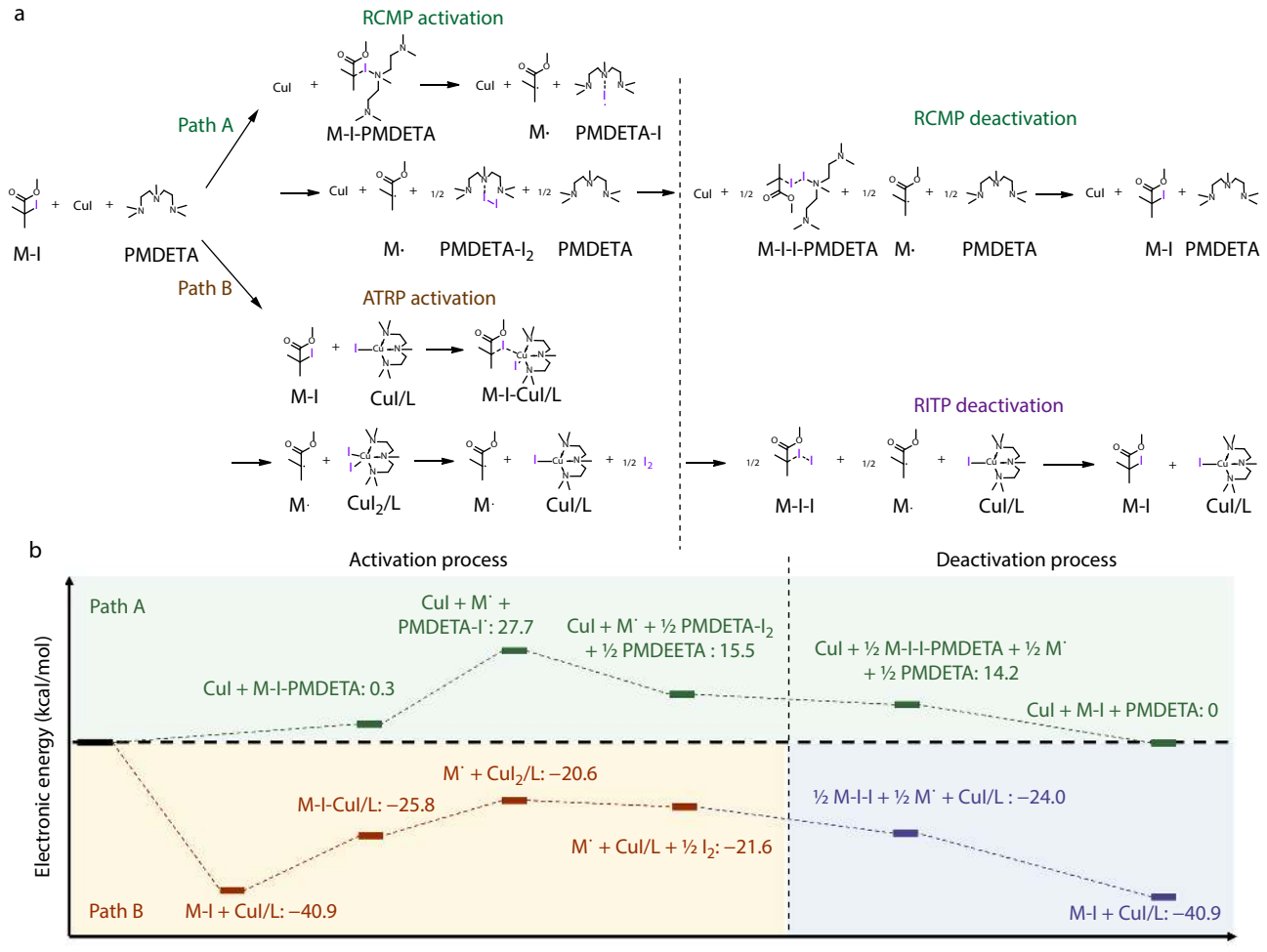

https://doi.org/10.1007/s10118-026-3669-7

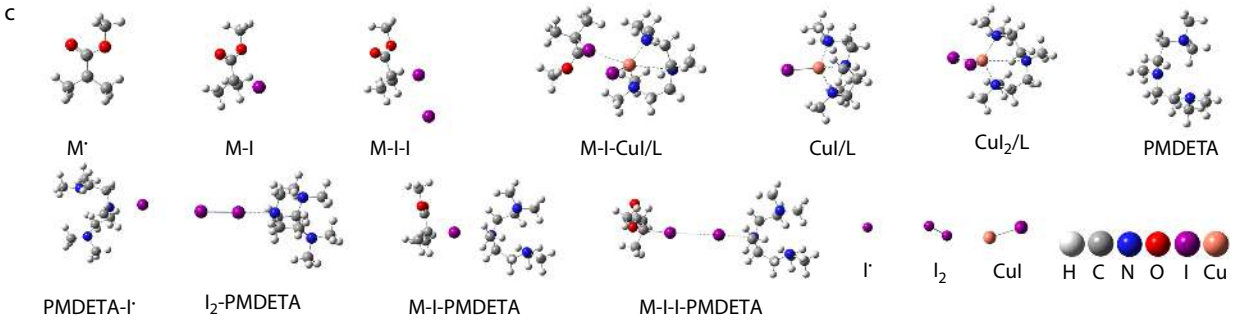

Fig. 6 DFT calculation for activation and deactivation pathways in the ternary RITP/RCMP/ATRP polymerization. (a) Demonstration of two reaction pathways: RCMP activation-deactivation (Path A) and CuI/L activation *via* ATRP-I_2 deactivation *via* RITP (Path B); (b) Free energy profiles for two pathways; (c) The structure of substrates used in two pathways.

the B3LYP functional combined with the def2-TZVP basis set for geometry optimization and frequency analysis.[65] Fig. 6(a) illustrates two possible pathways considered. Path A corresponds to the activation-deactivation cycle of the RCMP mechanism. During RCMP activation, PMDETA reversibly complexes with alkyl iodide (M-I) to generate propagating radicals (M•) and PMDETA-I•. Two PMDETA-I• species can subsequently recombine to generate PMDETA-I_2 and 1/2 PMDETA in a more stable form. As for deactivation, M• reacts with PMDETA-I_2 forming the dormant M-I. In contrast, Path B represents CuI/L activation through ATRP, and I_2 deactivation through RITP. In this pathway, dormant M-I is activated by CuI/L, forming M• along with the CuI_2/L complex. Owing to the intrinsic instability of CuI_2, the complex further decomposes into 1/2 I_2 and CuI/L. The *in situ* generated I_2 subsequently deactivates M• *via* RITP, regenerating dormant M-I.

The calculated energy profiles (Fig. 6b) reveal clear energetic preferences between the RCMP pathway and the proposed ATRP-RITP mechanism. During the activation stage, when M-I, CuI, and PMDETA are simultaneously present, ligand complexation preferentially occurs with CuI (ΔG=–40.9 kcal/mol) rather than with the M-I (ΔG=0.25 kcal/mol). This spontaneous complexation between PMDETA and CuI plays a decisive role in lowering the overall energy of the ATRP pathway relative to RCMP. Although the subsequent activation of dormant M-I species to form M• and CuI_2/L shows an increase in overall energy (ΔG=–20.6 kcal/mol), this energy level remains substantially lower than that of the RCMP activation pathway, which exhibits a much higher overall activation energy of 15.5 kcal/mol. Importantly, the CuI_2/L species is calculated to be thermodynamically unstable and decomposes into a more stable form of CuI/L and 1/2 I_2 (ΔG=–21.6 kcal/mol). This spontaneous decomposition provides a continuous source of I_2 for further RITP deactivation. In the deactivation stage, a similar energy preference is observed. Compared with the RCMP deactivation process mediated by PMDETA-I_2 (ΔG=14.2 kcal/mol), direct deactivation of M• by I_2 *via* the RITP mechanism is more favorable with overall deactivation energy of only –24.0 kcal/mol. In summary, these results suggest that activation of the dormant chain is more likely to proceed *via* the ATRP pathway through CuI/L, whereas radical deactivation proceeds preferentially through the RITP mechanism *via* I_2, ultimately leading to iodine-capped polymer terminals.

Chain Extensions and Block Polymer Synthesis

To demonstrate that the iodine terminal of the synthesized polymer remained active, chain extensions were carried out. As shown in Fig. 7, a macroinitiator is first synthesized and purified (M_n=3.6 kDa, $Đ$=1.10) and subsequently used to reinitiate MMA polymerization. To preserve the stability of the iodine terminal, the reaction was performed at 60 °C. The molar mass (M_n=29.3 kDa) of the resulting polymer increases with low dispersity ($Đ$=1.11, Conv.=50%) after 4 h. This proves that chain-end fidelity can be maintained. Based on this chain-extension experiment, the block polymer was synthesized using the same macroinitiator and polymerization conditions. The SEC traces in Fig. 7 show the successful synthesis of different block polymers with BMA (4 h, Conv.=50%), and BzMA (3 h, Conv.=37%) as the second block. This demonstrates the living characteristics of PMMA-I from the ternary RITP/RCMP/ATRP radical polymerization.

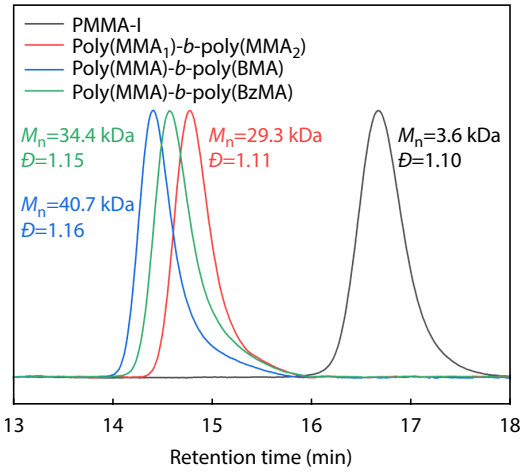

Fig. 7 SEC traces for macroinitiator, chain extension and block polymerization (black: PMMA-I, [MMA]:[I_2]:[ABVN]:[CuI]:[PMDETA] = 200:1:2:0.4:0.4; red: poly(MMA_1)-*b*-poly(MMA_2), [MMA]:[PMMA-I]:[CuI]:[PMDETA] = 500:1:2:2; green: poly(MMA)-*b*-poly(BzMA), [BzMA]:[PMMA-I]:[CuI]:[PMDETA] = 500:1:2:2; blue: poly(MMA)-*b*-poly(BMA), [BMA]:[PMMA-I]:[CuI]:[PMDETA] = 500:1:2:2.

CONCLUSIONS

In conclusion, this work proposes a ternary RITP/RCMP/ATRP

polymerization and systematically investigates the roles of each mechanism at different polymerization stages. RITP enables the *in situ* generation of CPI initiators, avoiding the use of unstable alkyl iodides. The introduction of ligands converts the RITP polymerization into a binary RCMP/RITP process, where the iodine-ligand complexation suppresses the generation of CPI but promotes its consumption, thereby accelerating polymerization. However, in the ternary RITP/RCMP/ATRP mechanism, the stronger complexation between copper and the ligand weakens the iodine-ligand interaction, leading to a lower rate of CPI activation and propagation, and a more controlled process compared with the binary RITP/RCMP mechanism. Kinetic and SEC studies reveal that a 1:1 ligand-to-copper ratio facilitates the full participation of CuI in the ATRP process and the livingness of polymerization. Furthermore, a mechanism of ATRP activation *via* CuI/L coupled with RITP deactivation *via* I_2 is proposed and verified by radical-trapping experiments and HPLC kinetic analysis, confirming that effective I_2 generation occurs in the presence of both copper and the ligand. DFT calculations further verified that dormant chain activation proceeds preferentially *via* the ATRP route through CuI/L, whereas deactivation proceeds predominantly *via* RITP through I_2, resulting in iodine-deactivated polymer ends. The obtained polymers retained high end-group fidelity, enabling successful chain extension and block copolymerization. This iodine-mediated radical polymerization enables the well-controlled polymerization of a broad range of methacrylate monomers and highlights the interplay among multiple regulation pathways, providing mechanistic insight into multi-mechanism RDRP polymerization.

Conflict of Interests

Xin-Yuan Zhu is an editorial board member for *Chinese Journal of Polymer Science* and was not involved in the editorial review or the decision to publish this article. The authors declare no interest conflict.

Electronic Supplementary Information

Electronic supplementary information (ESI) is available free of charge in the online version of this article at http://doi.org/10.1007/s10118-026-3669-7.

Data Availability Statement

The related data (DOI: 10.57760/sciencedb.j00189.00056) for this paper is available in the Science Data Bank (ScienceDB) database (https://www.scidb.cn/s/QZ7Bbe).

ACKNOWLEDGMENTS

X.Z. acknowledges the National Key Research and Development Program of China (No. 2023YFF0724100) and the National Natural Science Foundation of China (No. 52421006). N.R. acknowledges the State Key Laboratory of Polyolefins and Catalysis (No. SKLZX-2025-01).

REFERENCES

1 Wang, P.; Chen, S. J.; Cheng, J. N.; He, W. W.; Zhang, L. F.; Cheng, Z. P. Continuous synthesis of main-chain-type fluorinated graft copolymers *via* successive flow START polymerization and Cu(0)-mediated RDRP. *Chinese J. Polym. Sci.* **2023**, *41*, 1155–1161.
2 Parkatzidis, K.; Amez, L. D.; Truong, N. P.; Anastasaki, A. Cu(0)-RDRP of acrylates using an alkyl iodide initiator. *Polym. Chem.* **2023**, *14*, 1639–1645.
3 Kumru, B.; Antonietti, M. Emerging concepts in iodine transfer polymerization. *Macromol. Chem. Phys.* **2023**, *224*, 2200316.
4 Chen, Z. H.; Wang, X. Y.; Tang, Y. Reversible complexation mediated polymerization: an emerging type of organocatalytically controlled radical polymerization. *Polym. Chem.* **2022**, *13*, 2402–2419.
5 Wang, J. Y.; Ni, Y. Y.; Cheng, J. N.; Zhang, L. F.; Cheng, Z. P. Molar mass dispersity control by iodine-mediated reversible-deactivation radical polymerization. *Chinese J. Polym. Sci.* **2021**, *39*, 1155–1160.
6 Wang, C. G.; Chong, A. M. L.; Pan, H. M.; Sarkar, J.; Tay, X. T.; Goto, A. Recent development in halogen-bonding-catalyzed living radical polymerization. *Polym. Chem.* **2020**, *11*, 5559–5571.
7 Dadashi-Silab, S.; Szczepaniak, G.; Lathwal, S.; Matyjaszewski, K. Iodine-mediated photoATRP in aqueous media with oxygen tolerance. *Polym. Chem.* **2020**, *11*, 843–848.
8 Chen, Z. H.; Ma, Y.; Wang, X. Y.; Sun, X. L.; Li, J. F.; Zhu, B. H.; Tang, Y. Winning strategy for iron-based ATRP using *in situ* generated iodine as a regulator. *ACS Catal.* **2020**, *10*, 14127–14134.
9 Ni, Y. Y.; Zhang, L. F.; Cheng, Z. P.; Zhu, X. L. Iodine-mediated reversible-deactivation radical polymerization: a powerful strategy for polymer synthesis. *Polym. Chem.* **2019**, *10*, 2504–2515.
10 Lanzalaco, S.; Fantin, M.; Scialdone, O.; Galia, A.; Isse, A. A.; Gennaro, A.; Matyjaszewski, K. Atom transfer radical polymerization with different halides (F, Cl, Br, and I): is the process "living" in the presence of fluorinated initiators *Macromolecules* **2016**, *50*, 192–202.
11 Isse, A. A.; Lin, C. Y.; Coote, M. L.; Gennaro, A. Estimation of standard reduction potentials of halogen atoms and alkyl halides. *J. Phys. Chem. B* **2011**, *115*, 678–684.
12 Luo, Y., in *Comprehensive Handbook of Chemical Bond Energies*, CRC Press, Cleveland USA, **2007**, p. 211-253.
13 Cavallo, G.; Metrangolo, P.; Milani, R.; Pilati, T.; Priimagi, A.; Resnati, G.; Terraneo, G. The halogen bond. *Chem. Rev.* **2016**, *116*, 2478–601.
14 Zhang, J.; Goto, A. Rapid and versatile polymer-polymer coupling *via* iodide-thiol substitution click chemistry. *Polym. Chem.* **2025**, *16*, 3968–3976.
15 Wang, C. G.; Chong, A. M. L.; Lu, Y.; Liu, X.; Goto, A. Metal-free fast azidation by using tetrabutylammonium azide: effective synthesis of alkyl azides and well-defined azido-end polymethacrylates. *Chemistry* **2019**, *25*, 13025–13029.
16 Wang, C. G.; Goto, A. Solvent-selective reactions of alkyl iodide with sodium azide for radical generation and azide substitution and their application to one-pot synthesis of chain-end-functionalized polymers. *J. Am. Chem. Soc.* **2017**, *139*, 10551–10560.
17 Coessens, V.; Matyjaszewski, K. End group transformation of polymers prepared by ATRP, substitution to azides. *J. Macromol. Sci. Pure Appl. Chem*. **1999**, *A36*, 667–679.
18 Matyjaszewski, K.; Möller, M, in *Polymer Science: A Comprehensive Reference*, Elsevier, Amsterdam Netherlands, **2012**, p. 159-180.
19 David, G.; Boyer, C.; Tonnar, J.; Ameduri, B.; Lacroix-Desmazes, P.; Boutevin, B. Use of iodocompounds in radical polymerization. *Chem. Rev.* **2006**, *106*, 3936–3962.
20 Pfukwa, H.; Coetzee, C.; Johani, J.; Carstens, A.; Lederer, A.; Pasch, H. Aldehyde-functionalized polymers from the reverse iodine transfer polymerization of lignin-derivable compounds. *ACS Appl.*

Graphical Abstract

Iodine-mediated Atom Transfer Radical Polymerization Enabled by the Cooperative Reverse Iodine Transfer Polymerization and Reversible Complexation Mediated Polymerization

Meng-Qi Ge, Xin-Wei Chen, Liang Wu, Xiang-Yi Wang, Ning Ren, and Xin-Yuan Zhu

Shanghai Jiao Tong University

An iodine-mediated reversible deactivation radical polymerization (RDRP) integrating reverse iodine transfer polymerization (RITP), reversible complexation mediated polymerization (RCMP), and atom transfer radical polymerization (ATRP) enabled *in situ* generation of alkyl iodide initiators. Their cooperative interplay enables controlled polymerization of methacrylates and provides insight into multi-mechanism radical polymerization.

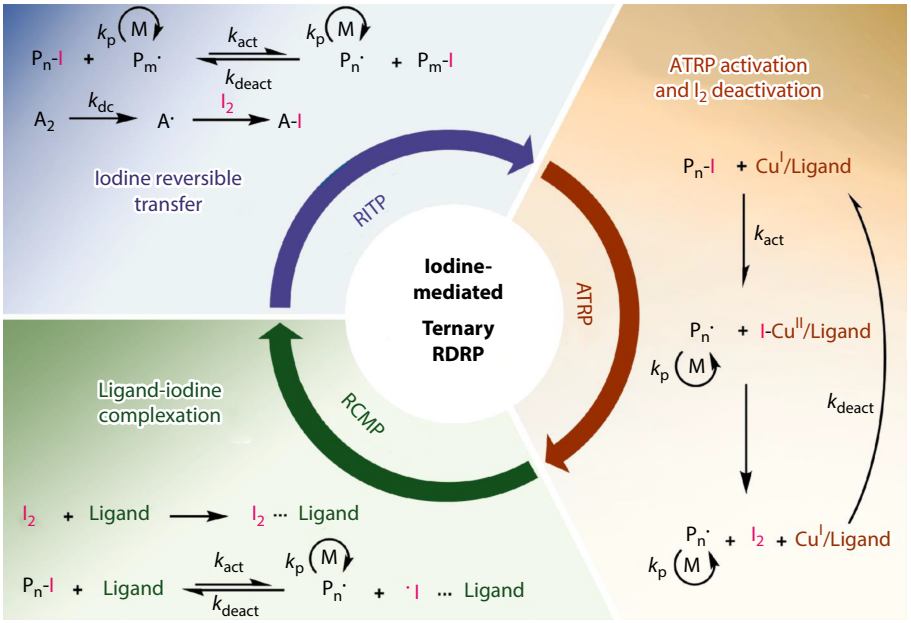

Chinese J. Polym. Sci., 2026 *https://doi.org/10.1007/s10118-026-3669-7*

Polym. Mater. **2021**, *3*, 3941–3952.
21 Huang, T.; Yuan, Q. X.; Gong, S. L. Emulsifier-free acrylate-based emulsion prepared by reverse iodine transfer polymerization. *Polymers* **2020**, *12*, 730.
22 Goto, A.; Suzuki, T.; Ohfuji, H.; Tanishima, M.; Fukuda, T.; Tsujii, Y.; Kaji, H. Reversible complexation mediated living radical polymerization (RCMP) using organic catalysts. *Macromolecules* **2011**, *44*, 8709–8715.
23 Sadakane, M.; Goto, A.; Harada, A.; Kitayama, Y. Impact of interfacial halogen bonding with a surfactant on miniemulsion reversible chain transfer-catalyzed polymerization. *Macromolecules* **2024**, *57*, 3338–3345.
24 Gao, D. N.; Zhao, Y. L.; Cai, J. Y.; Hou, L. X.; Xiao, L. Q. Reversible chain transfer catalyzed polymerization with alkyl iodides generated from alkyl bromides by halogen exchange. *Chinese J. Polym. Sci.* **2021**, *39*, 1161–1168.
25 Goto, A.; Tsujii, Y.; Fukuda, T. Reversible chain transfer catalyzed polymerization (RTCP): a new class of living radical polymerization. *Polymer* **2008**, *49*, 5177–5185.
26 Davis, K. A.; Matyjaszewski, K. Effect of (pseudo)halide initiators and copper complexes with non-halogen anions on the atom transfer radical polymerization. *J. Macromol. Sci. Pure Appl. Chem.* **2004**, *A41*, 449–465.
27 Lissi, E. A.; Aljaro, J. Methyl methactylate polymerization in the presence of iodine. *J. Polym. Sci. Polym. Lett. Ed.* **1976**, *14*, 499–502.
28 Ghosh, P.; Banerjee, A. N.; Mitra, P. S.; Chakraborty, S. Chain transfer in presence of halogens in the polymerization of methylmethacrylate. *J. Polym. Sci. Polym. Lett. Ed.* **1975**, *13*, 35–38.
29 Goto, A.; Zushi, H.; Hirai, N.; Wakada, T.; Kwak, Y.; Fukuda, T. Germanium- and tin-catalyzed living radical polymerizations of styrene and methacrylates. *Macromol. Symp.* **2007**, *248*, 126–131.
30 Goto, A.; Zushi, H.; Hirai, N.; Wakada, T.; TsOjii, Y.; Fukuda, T. Living radical polymerizations with germanium, tin, and phosphorus catalysts—reversible chain transfer catalyzed polymerizations (RTCPs). *J. Am. Chem. Soc.* **2007**, *129*, 13347–13354.
31 Goto, A.; Hirai, N.; Wakada, T.; Nagasawa, K.; Tsujii, Y.; Fukuda, T. Living radical polymerization with nitrogen catalyst: reversible chain transfer catalyzed polymerization with *N*-iodosuccinimide. *Macromolecules* **2008**, *41*, 6261–6264.
32 Goto, A.; Hirai, N.; Nagasawa, K.; Tsujii, Y.; Fukuda, T.; Kaji, H.

Phenols and carbon compounds as efficient organic catalysts for reversible chain transfer catalyzed living radical polymerization (RTCP). *Macromolecules* **2010**, *43*, 7971−7978.
33 Kitayama, Y.; Sadakane, M.; Harada, A. Reversible chain transfer catalyzed polymerization in miniemulsion systems with tetraiodomethane as a catalyst. *Polym. Chem.* **2022**, *13*, 6179−6186.
34 Vana, P.; Goto, A. Kinetic simulations of reversible chain transfer catalyzed polymerization (RTCP): guidelines to optimum molecular weight control. *Macromol. Theory Simul.* **2010**, *19*, 24−35.
35 Goto, A.; Hirai, N.; Tsujii, Y.; Fukuda, T. Reversible chain transfer catalyzed polymerizations (RTCPs) of styrene and methyl methacrylate with phosphorus catalysts. *Macromol. Symp.* **2008**, *261*, 18−22.
36 Wang, W. X.; Bai, L. J.; Chen, H.; Xu, H.; Niu, Y. Z.; Tao, Q.; Cheng, Z. P. PMDETA as an efficient catalyst for bulk reversible complexation mediated polymerization (RCMP) in the absence of additional metal salts and deoxygenation. *RSC Adv.* **2016**, *6*, 97455−97462.
37 Lei, L.; Tanishima, M.; Goto, A.; Kaji, H. Living radical polymerization *via* organic superbase catalysis. *Polymers* **2014**, *6*, 860−872.
38 Li, B.; Shi, Y.; Fu, Z. F. Schiff base as a novel kind of catalyst for reversible complexation-mediated radical polymerization of methyl methacrylate. *J. Polym. Sci., Part A: Polym. Chem.* **2019**, *57*, 1653−1663.
39 Wang, C. G.; Hanindita, F.; Goto, A. Biocompatible choline iodide catalysts for green living radical polymerization of functional polymers. *ACS Macro Lett.* **2018**, *7*, 263−268.
40 Sarkar, J.; Xiao, L.; Goto, A. Living radical polymerization with alkali and alkaline earth metal iodides as catalysts. *Macromolecules* **2016**, *49*, 5033−5042.
41 Goto, A.; Ohtsuki, A.; Ohfuji, H.; Tanishima, M.; Kaji, H. Reversible generation of a carbon-centered radical from alkyl iodide using organic salts and their application as organic catalysts in living radical polymerization. *J. Am. Chem. Soc.* **2013**, *135*, 11131−11139.
42 Xu, H.; Wang, C. G.; Lu, Y.; Goto, A. Pyridine *N*-oxide catalyzed living radical polymerization of methacrylates *via* halogen bonding catalysis. *Macromolecules* **2019**, *52*, 2156−2163.
43 Goto, A.; Tsujii, Y.; Kaji, H., in *Progress in Controlled Radical Polymerization: Mechanisms and Techniques*, American Chemical Society, Washington DC, **2012**, p. 305-315.
44 Tang, W.; Kwak, Y.; Braunecker, W.; Tsarevsky, N. V.; Coote, M. L.; Matyjaszewski, K. Understanding atom transfer radical polymerization: effect of ligand and initiator structures on the equilibrium constants. *J. Am. Chem. Soc.* **2008**, *130*, 10702−10713.
45 Tang, W.; Matyjaszewski, K. Effects of initiator structure on activation rate constants in ATRP. *Macromolecules* **2007**, *40*, 1858−1863.
46 Ford, M. C.; Waters, W. A. Properties and reactions of free alkyl radicals in solution. Part Ⅱ. Reactions with iodine, bromine, and sulphuryl chloride. *J. Chem. Soc.* **1951**, *1*, 1851−1855.
47 Chen, K. L.; Zhang, T.; Shi, Y.; Wang, Z. Y. Reversible complexation mediated polymerization (RCMP)-solution polymerization of methyl methacrylate catalyzed by $Bu_4N^+I^-$ (BNI) with *in situ* formed alkyl iodide initiator. *Mater. Res. Express* **2018**, *5*, 095310.
48 Goto, A.; Nagasawa, K.; Shinjo, A.; Tsujii, Y.; Fukuda, T. Reversible chain transfer catalyzed polymerization of methyl methacrylate with *in situ* formed alkyl iodide initiator. *Aust. J. Chem.* **2009**, *62*, 1492−1495.
49 Ohtani, K.; Shimizu, K.; Takahashi, T.; Takamura, M. Novel chain-end modification of polymer iodides *via* reversible complexation-mediated polymerization with functionalized radical generation agents. *Polymers* **2023**, *15*, 2667.
50 Borman, C. D.; Jackson, A. T.; Bunn, A.; Cutter, A. L.; Irvine, D. J. Evidence for the low thermal stability of poly(methyl methacrylate) polymer produced by atom transfer radical polymerisation. *Polymer* **2000**, *41*, 6015−6020.
51 Wright, T.; Chirowodza, H.; Pasch, H. NMR studies on the mechanism of reverse iodine transfer polymerization of styrene. *Macromolecules* **2012**, *45*, 2995−3003.
52 Lacroix-Desmazes, P.; Tonnar, J.; Boutevin, B. Reverse iodine transfer polymerization (RITP) in emulsion. *Macromol. Symp.* **2007**, *248*, 150−157.
53 Foldiak, G.; Schuler, R. H. Rate constants for the scavenging of radicals by iodine. *J. Phys. Chem.* **1978**, *82*, 2756−2757.
54 Bortolamei, N.; Isse, A. A.; Di Marco, V. B.; Gennaro, A.; Matyjaszewski, K. Thermodynamic properties of copper complexes used as catalysts in atom transfer radical polymerization. *Macromolecules* **2010**, *43*, 9257−9267.
55 Nagakura, S. Molecular complexes and their spectra. Ⅷ. The molecular complex between iodine and triethylamine1. *J. Am. Chem. Soc.* **1958**, *80*, 520−524.
56 Ren, N.; Wang, X. Y.; Sun, P.; Ge, M. Q.; Han, W. W.; Zhu, X. Y. Multi-mechanism polymerization as a promising tool for polymer synthesis. *Prog. Polym. Sci.* **2025**, *166*, 101988.
57 Ge, M. Q.; Wang, X. Y.; Ren, N.; Tong, G. S.; Zhu, X. Y. Multi-polymerization: from simple to complex. *Chinese J. Polym. Sci.* **2022**, *41*, 179−186.
58 Wang, X. Y.; Ren, N.; Ge, M. Q.; Chen, X. W.; Wu, L.; Zhu, X. Y. Binary copolymerization by ring-opening metathesis polymerization of norbornene-type/cyclooctene-type macromonomers. *ACS Appl. Polym. Mater.* **2025**, *7*, 8041−8054.
59 Chen, X. W.; Wu, L.; Wang, X. Y.; Ge, M. Q.; Ren, N.; Zhu, X. Y. Reactive molecular simulation and microscopic origins in the reaction kinetics of binary polymerization. *Macromolecules* **2025**, *58*, 4340−4356.
60 Zhang, S.; Ren, N.; Li, X.; Xiao, Y.; Lang, M.; Zhu, X. Y. RAFT/ROP binary polymerization towards well-defined graft copolymers. *Polym. Chem.* **2024**, *15*, 1992−2001.
61 Li, X.; Ren, N.; Xiao, Y.; Li, X.; Lang, M.; Zhu, X. Y. Construction and regulation on thiol-acrylate networks through binary polymerization of thiol-ene polymerization and free radical polymerization. *Macromolecules* **2024**, *57*, 9867−9876.
62 Ren, N.; Ge, M. Q.; Tong, G. S.; Zhu, X. Y. Advancing from unimechanism polymerization to multimechanism polymerization: binary polymerization. *Sci. Chi. Chem.* **2021**, *65*, 602−610.
63 Jazani, A. M.; Yilmaz, G.; Baumer, M.; Sobieski, J.; Bernhard, S.; Matyjaszewski, K. Unraveling the roles of amines in atom transfer radical polymerization in the dark. *J. Am. Chem. Soc.* **2025**, *147*, 12562−12573.
64 Xia, J.; Zhang, X.; Matyjaszewski. K., in *Transition Metal Catalysis in Macromolecular Design*, American Chemical Society, Washington DC, **2000**, p. 207−223.
65 Frisch, M. J.; Trucks, G. W.; Schlegel, H. B.; Scuseria, G. E.; Robb, M. A.; Cheeseman, J. R.; Scalmani, G.; Barone, V.; Mennucci, B.; Petersson, G. A.; Nakatsuji, H.; Caricato, M.; Li, X.; Hratchian, H. P.; Izmaylov, A. F.; Bloino, J.; Zheng, G.; Sonnenberg, J. L.; Hada, M.; Ehara, M.; Toyota, K.; Fukuda, R.; Hasegawa, J.; Ishida, M.; Nakajima, T.; Honda, Y.; Kitao, O.; Nakai, H.; Vreven, T.; Montgomery, J. A., Jr.; Peralta, J. E.; Ogliaro, F.; Bearpark, M.; Heyd, J. J.; Brothers, E.; Kudin, K. N.; Staroverov, V. N.; Kobayashi, R.; Normand, J.; Raghavachari, K.; Rendell, A.; Burant, J. C.; Iyengar, S. S.; Tomasi, J.; Cossi, M.; Rega, N.; Millam, N. J.; Klene, M.; Knox, J. E.; Cross, J. B.; Bakken, V.; Adamo, C.; Jaramillo, J.; Gomperts, R.; Stratmann, R. E.; Yazyev, O.; Austin, A. J.; Cammi, R.; Pomelli, C.; Ochterski, J. W.; Martin, R. L.; Morokuma, K.; Zakrzewski, V. G.; Voth, G. A.; Salvador, P.; Dannenberg, J. J.; Dapprich, S.; Daniels, A. D.; Farkas, Ö.; Foresman, J. B.; Ortiz, J. V.; Cioslowski, J.; Fox, D. J. Gaussian 16, Revision A.03. Gaussian Inc., Wallingford, CT 2016.